Analyst

RSC Publishing

COMMUNICATION

View Article Online
View Journal

A smart T_1-weighted MRI contrast agent for uranyl cations based on a DNAzyme–gadolinium conjugate†

Cite this: DOI: 10.1039/c3an01182h

Weichen Xu, Hang Xing and Yi Lu*

Received 14th June 2013
Accepted 10th August 2013

DOI: 10.1039/c3an01182h

www.rsc.org/analyst

Rational design of smart MRI contrast agents with high specificity for metal ions remains a challenge. Here, we report a general strategy for the design of smart MRI contrast agents for detecting metal ions based on conjugation of a DNAzyme with a gadolinium complex. The 39E DNAzyme, which has high selectivity for UO_2^{2+}, was conjugated to Gd(III)–DOTA and streptavidin. The binding of UO_2^{2+} to its 39E DNAzyme resulted in the dissociation of Gd(III)–DOTA from the large streptavidin, leading to a decrease of the T_1 correlation time, and a change in the MRI signal.

Metal ions play critical roles in many biological systems. However, the important and vital functions of many metal ions are often offset by toxicity when the metal ions are in excess or when non-physiological metal ions, such as heavy metal ions, are present. In order to achieve a deeper understanding of the mechanisms by which these metal ions exert their beneficial or deleterious effects, tools that can monitor these metal ions in biological systems are required. Toward this goal, tremendous effort has been applied towards developing different types of metal ion sensors, such as fluorescent, colorimetric, and electrochemical sensors.[1–12] Among them, magnetic resonance imaging (MRI) is unique, as it is the only type that allows non-invasive three-dimensional imaging *in vivo*. Critical to the success of this method is the development of MRI contrast agents, which are paramagnetic compounds such as Gd(III) chelates or superparamagnetic iron oxide nanoparticles, used to alter the magnetic relaxivity in different tissue types. Accordingly, a smart contrast agent is the combination of an MRI contrast agent with a selective reagent that allows for target detection by alternating the magnetic relaxivity.[13–17] Meade and coworkers pioneered this area by developing a smart contrast agent for the detection of Ca^{2+}.[18] Since that time, T_1-weighted smart contrast agents have been developed for the recognition of Ca^{2+},[19] Zn^{2+},[20,21] and Cu^{2+}.[22,23] However, the rational design of smart contrast agents with high specificity for a specific metal ion remains a significant challenge. First, it is difficult to design and synthesize molecules that can recognize different metal ions in their different oxidation states with high binding affinity and selectivity. Additionally, transforming the binding into an MRI signal without affecting the selectivity is not trivial.

In order to design smart MRI contrast agents for a wide range of metal ions, a target recognition domain with high selectivity and specificity must be combined with the imaging domain. However, the rational design of a gadolinium complex that is selective for one metal ion over others can be very challenging and oftentimes is the major roadblock to progress. To meet this challenge, the use of combinatorial selection processes can be applied. Metal ion-responsive DNAzymes are excellent candidates for this purpose.[24,25] DNAzymes are catalytic DNA molecules that are obtained through *in vitro* selection or Systematic Evolution of Ligands by Exponential Enrichment (SELEX) from a large random DNA library consisting of up to 10^{15} different sequences.[26–30] The broad range of sequence space allows for a wide variety of secondary and tertiary structures, enabling a large range of possible reactivities including catalyzing RNA hydrolysis,[31] Diels–Alder reaction,[32,33] and dephosphorylation.[34] A powerful advantage of the use of DNAzymes is that the selection conditions may be controlled to find DNAzymes specific for a particular metal ion of interest, without advance knowledge of what specific sequence or binding motif is necessary. Finally, DNA is relatively simple to synthesize and modify, and thus once a DNAzyme is selected, the modification of that DNAzyme for different signal outputs is straightforward. As a result, a number of DNAzymes have been selected, and developed into fluorescent, colorimetric, and electrochemical sensors.[35–43] However, to date no smart MRI contrast agents based on DNAzymes have been reported.

In this work, we report a smart T_1-weighted MRI contrast agent for uranyl, based on the conjugation of a uranyl-selective DNAzyme with a Gd–DOTA contrast agent. Since DNAzymes can

Department of Chemistry, University of Illinois at Urbana-Champaign, Urbana, Illinois 61801, USA. E-mail: yi-lu@illinois.edu; Fax: +1-217-244-3186; Tel: +1-217-333-2619

† Electronic supplementary information (ESI) available. See DOI: 10.1039/c3an01182h

be selected for any metal ion of interest, and the conjugation chemistry and signal transduction can be applied to any DNAzyme system, this method can be used for development of smart MRI contrast agents for a wide variety of metal ions and can thus help expand our understanding of the role of metal ions in biology.

In order to develop a smart MRI contrast agent with switchable relaxivity in response to the presence of uranyl, a uranyl-selective 39E DNAzyme is chosen to combine with MRI imaging agent Gd–DOTA. The 39E DNAzyme consists of an enzyme strand called 39E, which is able to catalyze the hydrolysis of a substrate strand called 39S, containing a scissile ribonucleotide adenosine (rA) in the middle (Fig. 1).[44,45] This DNAzyme was isolated through *in vitro* selection and has a high binding affinity for UO_2^{2+} (K_d = 463 nM). Because of these properties, the 39E DNAzyme has also been developed into fluorescent and colorimetric sensors for UO_2^{2+} with detection limits down to 45 pM, and selectivity of more than a million fold.

The design of the 39E DNAzyme-based smart MRI contrast agent is shown in Fig. 1. The enzymatic strand 39E (green) contains a biotin at its 3′ end, which is used to couple to streptavidin. The Gd–DOTA is attached to the 5′ end of the substrate strand 39S (black) through an amine–carboxylic acid coupling reaction (*vide infra*). At ambient temperature, these two strands are hybridized forming a stable structure containing the large streptavidin protein, because the melting temperature of the two DNA strands is above room temperature. In the presence of UO_2^{2+}, however, the DNAzyme can cleave the 39S strand. The resulting shorter fragments have lower melting temperature, which is below ambient temperature, thus allowing a release of the cleaved 39S strand containing the Gd–DOTA from the enzyme strand and the large streptavidin with high molecular weight. Based on Solomon–Bloembergen–Morgan theory, the relaxivity of the gadolinium compound is regulated by the rotation correlation time.[13] Since larger molecules have longer rotation correlation time, changing the size of the gadolinium compound leads to a change of its relaxivity.[46] Therefore, after the cleavage and release of the 39S strand, the relaxivity of Gd–DOTA associated with the much smaller cleaved product is changed, indicating the presence of uranyl cations. We have previously used a similar principle in developing a smart MRI contrast agent system for adenosine.[47] Compared with previously reported smart MRI contrast agents based on superparamagnetic iron oxide nanoparticles,[48,49] the Gd–DOTA-based contrast agent is smaller and, therefore easier to use for potential intracellular imaging.

To our knowledge, the activity of 39E has not been reported at high concentrations of streptavidin. As streptavidin may bind to UO_2^{2+} non-specifically and affect the activity of the DNAzyme, it is important to test the activity of the 39E DNAzyme in the presence of streptavidin. To perform the experiment, 30 μM of the 39E DNAzyme and carboxyfluorescein-labeled 39S were dissolved in 50 mM MES–Na (pH 5.5) buffer. The solution was heated up to 90 °C and cooled to ambient temperature over one hour. Streptavidin was added into the solution at a concentration of 30 μM. The solution was incubated with different concentrations of the uranyl cation ranging from 0.2 to 10 μM for 30 min. The reaction was then quenched upon the addition of 8 M urea and 100 mM EDTA and the product was analyzed by denaturing gel electrophoresis. As shown in Fig. 2, in the presence of 0.2 μM uranyl, only a very small amount of 39S was cleaved. When the uranyl concentration increased to 0.5 μM, ~20% 39S was cleaved. The percentage of cleavage further increased to ~65% with the incubation of 10 μM uranyl. Although the activity of 39E decreases in the presence of a high concentration of streptavidin when compared to previously reported results, the 39E DNAzyme remains fully functional and can be used for quantitative detection of UO_2^{2+}.

The DOTA was first conjugated to the 5′ end of the amine modified DNA strand through an amine–carboxylic acid coupling reaction (Fig. 3). In a typical reaction, NHS activated DOTA was dissolved in acetonitrile at a concentration of 0.5 mg μL^{-1}. Modified DNA strands were dissolved in 50 mM carbonate buffer (pH 10) at a concentration of 25 μM. Aliquots of the NHS–DOTA solution (4 μL) were added into 1 mL DNA solution once per hour for five hours. During the synthesis process, the mixture was shaken gently at 4 °C. The mixing was continued for another 3 to 5 hours after the final addition. The product was then desalted on a C-18 cartridge (Sep-Pak,

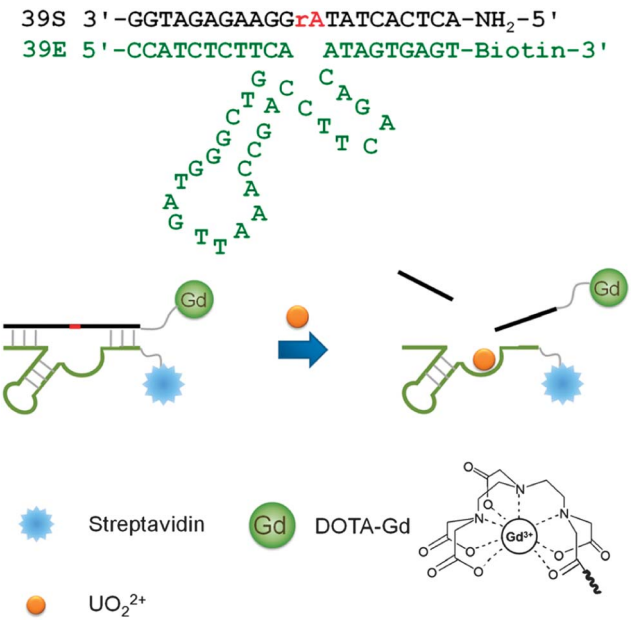

Fig. 1 Schematic view of the 39E DNAzyme-based smart MRI contrast agent for the sensing of UO_2^{2+}.

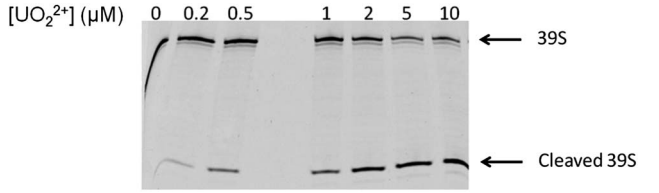

Fig. 2 Activity assay of 30 μM 39E DNAzyme in the presence of 30 μM streptavidin.

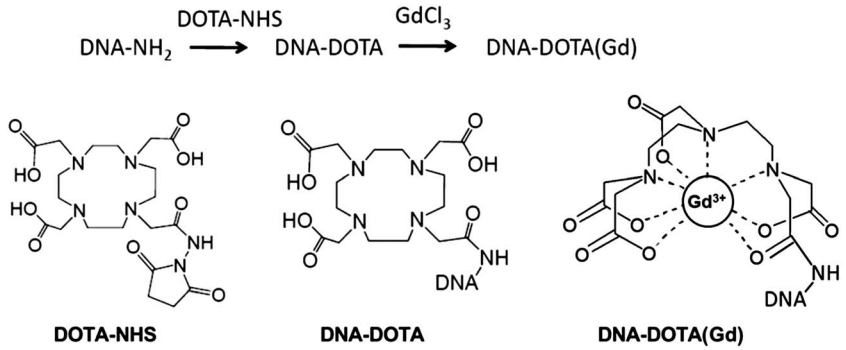

Fig. 3 Conjugation of the DOTA ligand to DNA and incorporation of Gd(III) into the DOTA–DNA conjugate.

Waters) and checked by MALDI-MS. A typical yield for conjugated DNA with less than 20 bases is 85–95%. It is critical to keep the entire synthesis free from metal contamination, as DOTA is a strong chelator for almost all metal cations.

To incorporate Gd(III) into the above DOTA–DNA conjugate, the DOTA conjugated DNA was dissolved in 50 mM acetate buffer (pH 5.55) at a concentration of 150 μM; $GdCl_3$ solution (10 mM) was added until the concentration reached 180 μM. $GdCl_3$ and DNA–DOTA solutions were mixed slowly and evenly to avoid precipitation. The solution was then kept at 75 °C for 30–45 min, and the final product was purified by size exclusion chromatography (PD10, GE Health Care Life Sciences) and lyophilized.

To investigate whether such synthesized DNAzyme-based smart contrast agents can be used for quantitative MRI sensing of UO_2^{2+}, the T_1 relaxation time of the 39E smart contrast agent was measured after incubation with different concentrations of UO_2^{2+}. As shown in Fig. 4a, the T_1 relaxation time increased from 1.55 s in the absence of UO_2^{2+}, to almost 2 s when 2 μM UO_2^{2+} was present. Higher concentrations of UO_2^{2+} resulted in longer T_1 relaxation times. The T_1 calibration curve had a logarithmic shape and reached saturation when the concentration of UO_2^{2+} was above 2 μM. These results suggest that the 39E DNAzyme-based smart MRI contrast agent can respond to UO_2^{2+} quantitatively and that the detection range of this agent is from 0.2 μM to 2 μM.

Furthermore, the selectivity of the smart MRI contrast agent was investigated by measuring the T_1 response to 10 μM of different metal ions. As shown in Fig. 4b, among all the metal ions tested, including UO_2^{2+}, Cd^{2+}, Hg^{2+}, Pb^{2+} and Zn^{2+}, only UO_2^{2+} resulted in a significant increase of T_1 of 0.35 s. Without UO_2^{2+}, or with other metal cations, no significant T_1 change was observed. The T_1 response of different metal ions suggests good selectivity of the smart MRI contrast agent.

In conclusion, we have designed and demonstrated the smart T_1-weighted MRI contrast agent for uranyl detection based on the 39E DNAzyme. It exhibits T_1 response to uranyl quantitatively and selectively. As different DNAzymes for a wide range of metal ions are achievable through *in vitro* selection, the method shown here can be applied to other metal ions based on an appropriate choice of DNAzyme.

This work was supported by the U.S. National Institutes of Health (ES16865) and the Department of Energy (DE-FG02-08ER64568). We wish to thank Drs. Thomas Meade, Keith MacRennaris, and Ying Song of Northwestern University for helpful discussions and the use of their relaxometer,

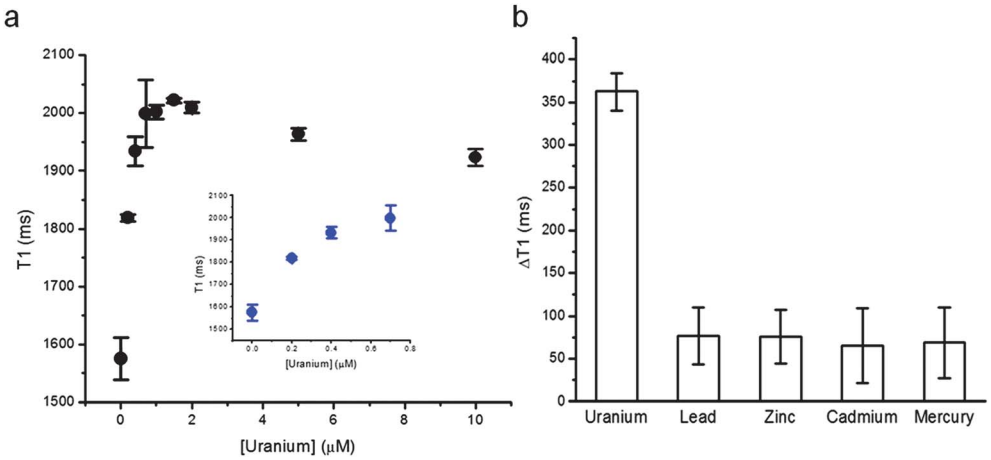

Fig. 4 (a) T_1 response of the 39E DNAzyme-based smart contrast agent to UO_2^{2+} at varying concentrations. The inset shows the T_1 response at low UO_2^{2+} concentrations. (b) Selectivity of the 39E DNAzyme-based smart contrast agent towards 10 μM of different divalent metal ions. The T_1 increase can only be observed when UO_2^{2+} is present.

Dr. Edward Treadwell of Eastern Illinois University for the use of his 60 MHz NMR spectrometer, and Ms Nancy Dodge for the acquisition of the MRI signals.

Notes and references

1 J. Zhang, R. E. Campbell, A. Y. Ting and R. Y. Tsien, *Nat. Rev. Mol. Cell Biol.*, 2002, **3**, 906–918.
2 E. L. Que, D. W. Domaille and C. J. Chang, *Chem. Rev.*, 2008, **108**, 1517–1549.
3 R. McRae, P. Bagchi, S. Sumalekshmy and C. J. Fahrni, *Chem. Rev.*, 2009, **109**, 4780–4827.
4 J. W. Liu, Z. H. Cao and Y. Lu, *Chem. Rev.*, 2009, **109**, 1948–1998.
5 T. Li, S. Dong and E. Wang, *Anal. Chem.*, 2009, **81**, 2144–2149.
6 T. Li, E. Wang and S. Dong, *Anal. Chem.*, 2010, **82**, 1515–1520.
7 J. Liu, J. Karpus, S. V. Wegner, P. R. Chen and C. He, *J. Am. Chem. Soc.*, 2013, **135**, 3144–3149.
8 M. D. Pluth, E. Tomat and S. J. Lippard, *Annu. Rev. Biochem.*, 2011, **80**, 333–355.
9 E. Tomat and S. J. Lippard, *Curr. Opin. Chem. Biol.*, 2010, **14**, 225–230.
10 S. V. Wegner, H. Arslan, M. Sunbul, J. Yin and C. He, *J. Am. Chem. Soc.*, 2010, **132**, 2567–2569.
11 S. V. Wegner, F. Sun, N. Hernandez and C. He, *Chem. Commun.*, 2011, **47**, 2571–2573.
12 P. Jiang and Z. Guo, *Coord. Chem. Rev.*, 2004, **248**, 205–229.
13 P. Caravan, J. J. Ellison, T. J. McMurry and R. B. Lauffer, *Chem. Rev.*, 1999, **99**, 2293–2352.
14 T. J. Meade, A. K. Taylor and S. R. Bull, *Curr. Opin. Neurobiol.*, 2003, **13**, 597–602.
15 K. Kikuchi, *Chem. Soc. Rev.*, 2010, **39**, 2048–2053.
16 P. Caravan, *Acc. Chem. Res.*, 2009, **42**, 851–862.
17 L. M. De Leon-Rodriguez, A. Ortiz, A. L. Weiner, S. R. Zhang, Z. Kovacs, T. Kodadek and A. D. Sherry, *J. Am. Chem. Soc.*, 2002, **124**, 3514–3515.
18 W. H. Li, S. E. Fraser and T. J. Meade, *J. Am. Chem. Soc.*, 1999, **121**, 1413–1414.
19 W. H. Li, G. Parigi, M. Fragai, C. Luchinat and T. J. Meade, *Inorg. Chem.*, 2002, **41**, 4018–4024.
20 K. Hanaoka, K. Kikuchi, Y. Urano and T. Nagano, *J. Chem. Soc., Perkin Trans. 2*, 2001, 1840–1843.
21 K. Hanaoka, K. Kikuchi, Y. Urano, M. Narazaki, T. Yokawa, S. Sakamoto, K. Yamaguchi and T. Nagano, *Chem. Biol.*, 2002, **9**, 1027–1032.
22 E. L. Que and C. J. Chang, *J. Am. Chem. Soc.*, 2006, **128**, 15942–15943.
23 E. L. Que, E. Gianolio, S. L. Baker, A. P. Wong, S. Aime and C. J. Chang, *J. Am. Chem. Soc.*, 2009, **131**, 8527–8536.
24 R. R. Breaker and G. F. Joyce, *Chem. Biol.*, 1994, **1**, 223–229.
25 R. R. Breaker, *Nat. Biotechnol.*, 1997, **15**, 427–431.
26 A. D. Ellington and J. W. Szostak, *Nature*, 1990, **346**, 818–822.
27 C. Tuerk and L. Gold, *Science*, 1990, **249**, 505–510.
28 R. R. Breaker, *Curr. Opin. Chem. Biol.*, 1997, **1**, 26–31.
29 S. W. Santoro and G. F. Joyce, *Proc. Natl. Acad. Sci. U. S. A.*, 1997, **94**, 4262–4266.
30 L. C. Bock, L. C. Griffin, J. A. Latham, E. H. Vermaas and J. J. Toole, *Nature*, 1992, **355**, 564–566.
31 J. Li and Y. Lu, *J. Am. Chem. Soc.*, 2000, **122**, 10466–10467.
32 M. Kurz and R. R. Breaker, *Curr. Top. Microbiol. Immunol.*, 1999, **243**, 137–158.
33 M. Chandra and S. K. Silverman, *J. Am. Chem. Soc.*, 2008, **130**, 2936–2937.
34 J. Chandrasekar and S. K. Silverman, *Proc. Natl. Acad. Sci. U. S. A.*, 2013, **110**, 5315–5320.
35 Z. J. Liu, S. H. J. Mei, J. D. Brennan and Y. F. Li, *J. Am. Chem. Soc.*, 2003, **125**, 7539–7545.
36 Y. Xiao, A. A. Rowe and K. W. Plaxco, *J. Am. Chem. Soc.*, 2007, **129**, 262–263.
37 M. Hollenstein, C. Hipolito, C. Lam, D. Dietrich and D. M. Perrin, *Angew. Chem., Int. Ed.*, 2008, **47**, 4346–4350.
38 T. Li, S. J. Dong and E. Wang, *Anal. Chem.*, 2009, **81**, 2144–2149.
39 B. C. Yin, B. C. Ye, W. H. Tan, H. Wang and C. C. Xie, *J. Am. Chem. Soc.*, 2009, **131**, 14624–14625.
40 T. Lan, K. Furuya and Y. Lu, *Chem. Commun.*, 2010, **46**, 3896–3898.
41 Z. D. Wang and Y. Lu, *J. Mater. Chem.*, 2009, **19**, 1788–1798.
42 H. Xing, N. Y. Wong, Y. Xiang and Y. Lu, *Curr. Opin. Chem. Biol.*, 2012, **16**, 429–435.
43 P. Wu, K. Hwang, T. Lan and Y. Lu, *J. Am. Chem. Soc.*, 2013, **135**, 5254–5257.
44 J. W. Liu, A. K. Brown, X. L. Meng, D. M. Cropek, J. D. Istok, D. B. Watson and Y. Lu, *Proc. Natl. Acad. Sci. U. S. A.*, 2007, **104**, 2056–2061.
45 A. K. Brown, J. W. Liu, Y. He and Y. Lu, *ChemBioChem*, 2009, **10**, 486–492.
46 P. Caravan, C. T. Farrar, L. Frullano and R. Uppal, *Contrast Media Mol. Imaging*, 2009, **4**, 89–100.
47 W. C. Xu and Y. Lu, *Chem. Commun.*, 2011, **47**, 4998–5000.
48 M. V. Yigit, D. Mazumdar, H. K. Kim, J. H. Lee, B. Dintsov and Y. Lu, *ChemBioChem*, 2007, **8**, 1675–1678.
49 M. V. Yigit, D. Mazumdar and Y. Lu, *Bioconjugate Chem.*, 2008, **19**, 412–417.

